Experimental search for phenomena at low energies beside Standard model

A.V.Derbin, A.I.Egorov, V.N.Muratova, S.V.Bakhlanov

1. Introduction

Standard model successfully described all the physical phenomena up to recent time. But recent discovery of oscillations of atmospheric neutrino shows that minimal Standard model has to be extended. The main trends are connected with determination of neutrino properties, including masses and mixing angles, search for double beta decay and a problem of hidden mass of Galaxy. Below the main results obtained by Group of low background measurements in this field of research are presented.

2. Restriction on the Magnetic Dipole Moment of Reactor Neutrinos

The puzzle of solar neutrino registered by Homestake, SAGE, GALLEX and Kamiokande detectors was explained by the fact that the interaction of the magnetic moment of the neutrino with the magnetic field of the Sun leads to a reversal of neutrino helicity [1], and right neutrinos do not participate in the reaction of charged currents. The value of the magnetic moment required for the observation of such variations of the left neutrino flux lies in the range of $10^{-10} – 10^{-11}$ electron Bohr magneton ($\mu_B=e/2m_e$).

This value of the magnetic moment is six or seven orders of magnitude higher than the value predicted by the standard theory, but does not contradict the restrictions obtained in laboratory experiments. Elastic scattering of a neutrino by an electron turns out to be the most sensitive to the magnetic moment [2-7]. The measured values of the cross section of this process set the restriction $\mu_\nu \le (1.5 - 4.0)\times10^{-10}\mu_B$ on the possible magnetic moment for electron antineutrinos, and $\mu_\nu \le 10.8\times10^{-10}\mu_B$ for electron neutrinos, and $\mu_\nu \le (7.4 – 9.5)\times10^{-10}\mu_B$ for muon neutrinos. The restrictions on the magnetic moment for electron antineutrinos were obtained from a reactor experiment, while those for electron and muon neutrinos result from experiments at accelerators.

The magnetic moment of the neutrino has a long history beginning from the Pauli hypothesis and the first calculations of the cross section of (ν_e,e) scattering. For a long time, the negative results of experiments on the search for neutrino-electron interaction were interpreted as a limitation on a possible magnetic moment of the neutrino. In Standard model, scattering of a neutrino possessing a magnetic moment is determined both by weak interaction and by the one-photon exchange. The amplitudes of weak and magnetic scattering do not interfere, and the total cross section is only the sum of the cross sections. The contribution of the magnetic moment is negligibly small in Standard model.

The differential cross section of weak scattering of an electron antineutrino in the Standard theory has the form:

$$\frac{d\sigma}{dE} = \frac{2G^2 m_e}{\pi}\left(g_R^2 + g_L^2\left(1-\frac{E_e}{E_\nu}\right)^2 - g_L g_R \frac{m_e E_e}{2E_\nu^2}\right.$$

where $G^2m_e/2\pi = 4.28 \times 10^{-45}$ cm^2/MeV, the values of g_R and g_L depend only on the Weinberg angle $g_R = sin^2\theta_w$, $g_L = ½ + sin^2\theta_w$, and E_ν and E_e are energies of the incident neutrino and the recoil electron. On the contrary, the neutrino scattering cross section associated with the magnetic moment is proportional to μ^2:

$$\frac{d\sigma}{dE} = \mu^2 \pi r_0^2 \left(\frac{1}{E_e} - \frac{1}{E_\nu}\right)$$

where μ is measured in Bohr magnetons and $r_0 = 2.818\times10^{-13}$ cm is the classical electron radius. The energy dependences of the cross sections of magnetic and weak scattering differ considerably. For $E_e \le E_\nu$ their ratio is proportional to $1/E_e$, i.e., a reduction of the electron detection threshold must increase the sensitivity of the experiment to the magnetic moment if the background increases slower than $lnE_e/_e$. The complexity of the experiment lies in the facts that the reaction cross section is small ($\approx10^{-44}$ cm^2), the only detectable particle is the recoil electron and the detector background increases at low energies. As a

result, the admissible effect-to-background ratio can be obtained only for a wide and a single range of the recoil electron. The theoretical predictions can be compared with experimental results only after averaging cross sections over the neutrino spectrum $N(E_\nu)$ as well as over the energy interval in which the electron is detected. The spectrum of antineutrino $N(E_\nu)$, is an independent problem in reactor experiments [8]. Now three research groups have measured the cross section of reactor neutrino-electron scattering in six different intervals of recoil electron energy. These results can be presented in the units of the weak scattering cross-section (fig.1). Although five of six results correlate with the Standard theory to within experimental error, all of them deviate toward larger cross sections. If we take the quantity $(\sigma_{exp} - \sigma_{weak}) + \Delta\sigma_{exp}$ for determining the upper bound of possible magnetic moment, the obtained values range from 1.4 and 3.4 in the 10^{-10} μ_B units. Using maximum likelihood method one can find that the upper limit on the neutrino magnetic moment, obtained from experiments with reactor neutrinos, is 1.5×10^{-10} μ_B (90% c.l).

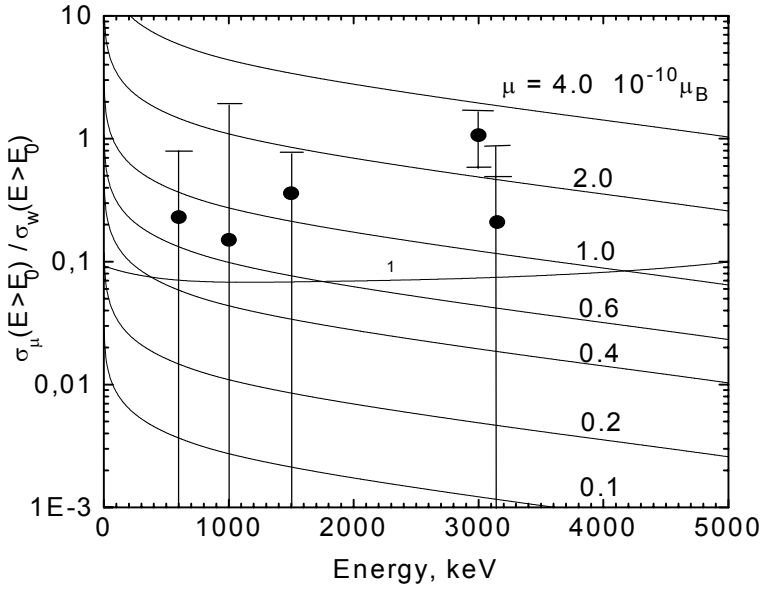

Fig.1. Ratio of the total cross sections of magnetic and weak scattering in the energy interval from threshold energy to 9 MeV for various values of magnetic moment (in 10^{-10} μ_B units). The experimental results of Savana River, Rovno and Krasnoyarsk (with errors) obtained under the assumption that the deviation of σ_{exp} from σ_{weak} is associated with the magnetic moment are indicated.

3. Search for Heavy Neutrino Emitted in Nuclear β-decay

Whether the mass and current states of neutrinos are identical is one of the most pressing problems in elementary particle physics. Up to recent time a search for neutrino oscillations at reactors and accelerators, on the one hand, and an analysis of the kinematics of two- and three-particle decays accompanied by neutrino emission, on the other hand, has so far yielded no more than limitations on the masses and mixing angles.

3.1. The 17 keV Neutrino in the ^{63}Ni β-decay

In 1985-86 J.J.Simpson from an analysis of β-spectrum of ^{3}H claimed about existing heavy neutrino with mass 17 keV and a mixing probability of 0.03-0.01 [9]. Later this result was confirmed by seven research groups; all of them used semiconductor detectors to measure the electron energy in β-decay or bremsstrahlung photon energy. It stands in clear contradiction with the data of corresponding experiments that used magnetic spectrometers. The reliability of the interpretation of these experiments depends on how well the response function of the detector is known.

In our study [10] a thin layer of ^{63}Ni ($T_{1/2} \approx 100$ yr, $E_0 \approx 67$ keV) was deposited directly on the gold coating of a Si(Li) detector. This detector was pressed tightly, without any gap, against the second,

identical detector, and a bias voltage was applied to the common *p*-type contact. In this geometry, with the detectors connected in anticoincidence, the contribution of backscattering electrons to the low-energy part of the response function of the detectors was effectively suppressed. So the magnitude and the shape of the tail of the resolution function in our case are different from those which gave positive results for existence 17 keV neutrino. The way by which this tail was actually taken into account may be the reason for discrepancies between results obtained on semiconductor and magnetic spectrometers.

The ^{63}Ni working source, 5 mm in diameter, with an activity of 3.6×10^3 Bq, was deposited on the gold surface of a Si(Li) detector by electrolysis. After the nickel was deposited, the detectors were connected tightly together, were placed in a cryostat, and were cooled to liquid-nitrogen temperature. Both detectors had similar spectrometric channels. The resolution measured with the help of the 59 keV γ lines of ^{241}Am was 1.1 keV and the discrimination threshold for selection of coincident events was set 3 keV. Measurements were continued until a statistical base of 1.1×10^7 events/keV was built up near 50 keV.

The experimental spectrum of ^{63}Ni β-particles was compared with the theoretical spectrum by searching for a minimum of the functional χ^2. The expected spectrum of β-particles was presented as a sum of two usual β-spectrum (S) with weights proportional to mixing angles (U_{eH}):

$$S = (1-|U_{eH}|^2 S(M_\nu=0) + |U_{eH}|^2\, S(M_\nu=17 \text{ keV})$$

The distribution of values of χ_i with the parameters obtained from optimum fit at a fixed value $|U_{eH}|^2 = 0$ is shown in the upper part of fig.2 (χ^2_n=1.39). The results of the optimum fit for the fixed values of $|U_{eH}|^2$=0.01 and M_ν=17 keV are shown in the lower part of fig.2. The value χ^2_n=12.3 found here contradicts the results which support the existence of a heavy 17 keV neutrino. Using a dependence χ^2 on $|U_{eH}|^2$ we found that $|U_{eH}|^2 \le 0.0015$ at the 90 % confidence level. This value ss close to the upper limits found in experiments with magnetic spectrometers on the mixing parameter ($|U_{eH}|^2 \le 0.003$ for ^{63}Ni and $|U_{eH}|^2 \le 0.0017$ for ^{35}S), and it is in substantial contradiction to the mean value of ($|U_{eH}|^2$ = 0.0085±0.001) obtained in works with semiconductor detectors.

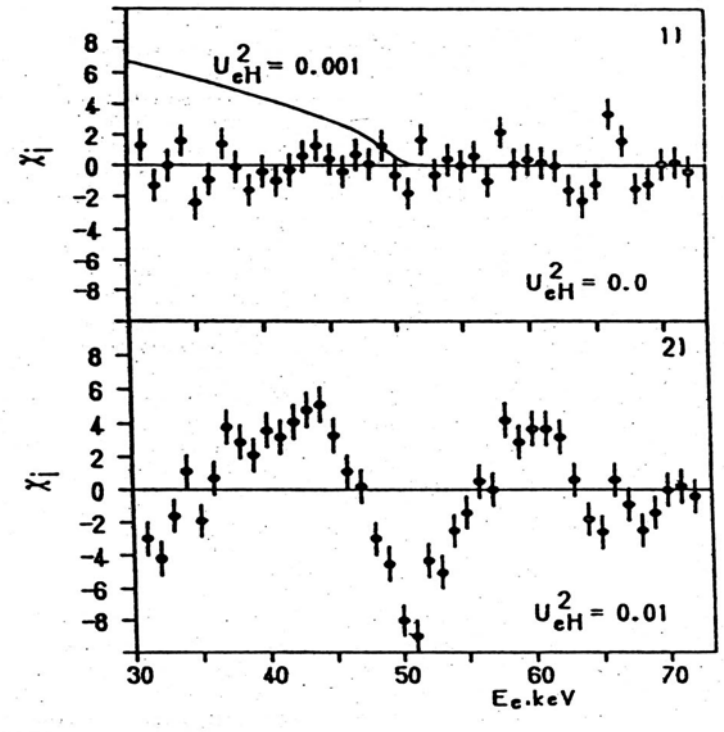

Fig.2. Results of optimal fit of β-spectrum of ^{63}Ni for m_ν= 0, $|U_{eH}|^2$=0 (upper part) and m_ν=17 keV, $|U_{eH}|^2$=0.01 (lower part). The solid line shows additional part connected with m_ν=17 keV, $|U_{eH}|^2$=0.001 (without fitting procedure).

3.2 Measurement of ^{45}Ca β-spectrum in Search for Deviation from the Theoretical Shape

In work [11] we analyzed the shape of β-spectrum of ^{45}Ca ($T_{1/2} \approx 164$ d, $E_0 \approx 256$ keV) which decays into the ^{45}Sc. The choice of isotope was dictated by our desire to check the model proposed in [12] for the appearance of a peak at the end of the β-spectrum [13], since the end-point energy of ^{45}Ca β-spectrum is very close to $m_e/2$. At the same time it makes possible to study the possibility of the emission of a neutrino with mass in the interval of 80-110 keV, for which the previously established limit did not exceed 10^{-2}.

The electrons were registered by Si(Li) detector having a sensitive region 12 mm in diameter and 3 mm high. A collimator-screened ^{45}Ca source was located at a distance of 25 mm from the detector surface. In this geometry the deviation of the resolution function from the Gaussian is mainly determined by the backscattering of electron detector surface as well as by electron energy losses in the source or the insensitive layer of the detector. To determine this function, the isotope of ^{125m}Te was added to ^{45}Ca and isotropically mixed with it. The experimentally determined resolution function of conversion electrons was used in the fitting procedure.

The total of 8×10^8 decays of ^{45}Ca were detected. To determine an additional part from the heavy neutrinos to the β-spectrum the maximum likelihood method was used in the same manner as was described above for 17 keV neutrinos. The fitting procedure gave acceptable value of χ^2 in the interval of electron energy 140-270 keV. The value of E_0 was determined to be 256.6(2) keV. The emission probability for different neutrino masses M_ν was determined by constructing a χ^2 profile. Fig.3 displays a curve of the limit on the probability of mixing of a heavy neutrino in the interval 20-160 keV (90 % c.l.) in comparison with other experiments. Therefore the new limit on the mixing parameter in the neutrino mass interval of 75-110 keV was obtained, $|U_{eH}|^2 \le 0.005$.

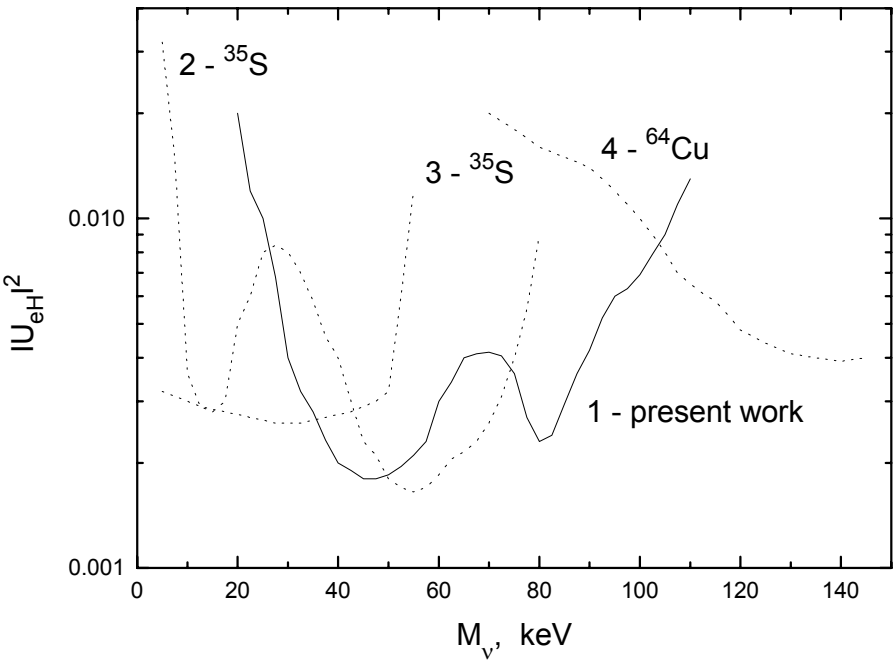

Fig.3. Limit on the mixing parameter $|U_{eH}|^2$ (90% confidence level) obtained in the present experiment (curve 1.) The curves 2,3 and 4 correspond to the limits obtained in ITEPh (Moscow) [14], CIT (California) [15] and ILL (Grenoble) [16].

The observation of a monochromatic peak in the continuous spectrum is a more model-independent problem than is the search for contribution from a smoothly increasing function in the case of the emission of a heavy neutrino. It was found that the probability for the appearance of a monochromatic peak near the end-point energy ($E_0 \pm 3$) keV is less than $(2.0 - 0.7)\times10^{-7}$ events per decay of ^{45}Ca. The limit on the intensity of the peak with energy equal to end-point energy (E_0) is equal to 1.3×10^{-7} (90%

c.l.). The achieved sensitivity to a monochromatic peak at the end of the β-spectrum is appreciably worse than the result obtained in [13]. But at the same time the limit obtained attests to the absence (at the level of 10^{-7}) of resonance end point peak enhancement due to the fact that $E_0=m_e/2$ [12].

4. Double β-decay (2β) to the Excited States of Daughter Nucleus

Recent direct measurements have shown that some nuclei may undergo two-neutrino double β-decay (2β2ν) with a half-life within 10^{18}–10^{21} yr. This discovery has given impetus extended search for 2β-decay processes, including those that occur to excited states of daughter nucleus [17]. Experimental data to be obtained will make it possible to estimate more accurately nuclear matrix elements and to set upper limits both on the neutrino mass and on other parameters neutrinoless double β-decay (2β0ν).

4.1 New Limits on Half-lives of ^{154}Gd, ^{160}Gd, ^{170}Er and ^{176}Yb with Respect to Double β-decay to the Excited 2^+ states

In study [18], we attempted to detect the 2β decay of ^{154}Gd, ^{160}Gd, ^{170}Er and ^{176}Yb nuclei, which were not investigated in this respect previously. For all daughter nuclei, the energy of the first excited 2^+ state lies between 80 and 120 keV. Therefore the reduction of the phase space suppresses insignificantly the probability of the 2β transition to this level. If we assume that the probability of 2β2ν-decay process is in direct proportion to the eleventh power of the transition energy, the probability e.g. of ^{160}Gd decay to the 2^+ level of ^{160}Dy is only twice as low as the probability of the decay to the ground state.

To count photons and to measure their energy, we used a coaxial germanium detector with a sensitive volume of 115 cm^3. The detection efficiency for photons in the range 80-120 keV was close to unity. The detector was placed in a special vacuum cryostat, whose design made it possible to reduce photon absorption in construction materials and to ensure a high geometric efficiency of counting. Samples of Sm, Gd, Er and Yb oxides were placed over the lateral and end-face surfaces of a titanium cup that enclosed the germanium crystal. The total area of the source was 200 cm^2. Absorption of photons in the oxide layer restricted the mass of each sample under study to 100 g. Within the cryostat the germanium detector was mounted on a copper cylinder which shielded the detector against the radioactivity of zeolite and elements of the electronics. The external passive shielding of the cryostat consisted of copper, mercury and lead. To suppress the background associated with cosmic rays, we used an active shielding consisting of five plastic scintillates.

Table 1

Limits on half-lives with respect to 2β(2ν+0ν) decay to the 2^+ states

Transition	Energy of the 2β-transition, keV	Energy of the 2^+, keV	Limit on $T_{1/2}$, yr (68 % c.l.)
^{154}Sm → ^{154}Gd	1250,0	123,07	≥ 2,3 10^{18}
^{160}Gd → ^{160}Dy	1731,1	86,79	≥ 6,5 10^{17}
^{170}Er → ^{170}Yb	654,2	84,26	≥ 3,2 10^{17}
^{176}Yb → ^{176}Hf	1076,9	88,35	≥ 1,6 10^{17}

As a result, the new limits on the half-lives with respect to 2β-decay to the 2^+ excited states of ^{154}Gd, ^{160}Dy, ^{170}Yb и ^{176}Hf nuclei have been established for ^{154}Sm, ^{160}Gd, ^{170}Er и ^{176}Yb nuclei. The sensitivity of the method used can be improved by reducing the background level and by increasing

sample masses and the time of measurements.

5. Search for Particles that Can Concern with Dark Matter of the Universe

5.1 Search for Invisible Axion in the Nuclear Magnetic Transitions

Theoretical models of invisible axion with the arbitrary scale of symmetry breaking up to the Planck mass serve as a basis for the experimental search for a pseudoscalar particle which interacts weakly with matter and whose mass ranges from 10^{-12} eV up to tens of keV [19,20]. Although the limits on the axion mass obtained from astrophysical estimates span almost the entire scale of possible masses, direct laboratory experiments give an upper limit of 6 keV for the axion mass. Models that include interactions of particles from a mirror world have found new window for axion mass ≈1 MeV that is not excluded by astrophysical data.

A new possibility for axion search is opened up using the method of missing γ-ray in nuclear magnetic transitions [21,22]. Assume «ideal» detector, which detects energy of all photons and electrons arising from the decay of a nucleus. But invisible axion leaves the detector without interactions. So this emission will be accompanied by a shift of the total energy spectrum by an amount equal to the transition energy. A study of magnetic transitions in isomeric nuclei is preferable [22], because there is no uncertainty associated with the emission of a neutrino for nuclei undergoing β and EC decay.

In works [22,23] we measured the energy spectrum of photons and electrons, arised in the decay of the ^{125m}Te nucleus. This isomeric nucleus undergoes M4 γ-transition with energy of 109.3 keV and M1 γ-transition with energy of 35.5 keV. The excited tellurium nucleus interacts with an atomic shell, with each decay of a nucleus being accompanied by a cascade of γ- and x-rays, conversion- and Auger electrons. As a model of «ideal» detector we used two cylindrical planar HPGe detectors butted together at their end gold surfaces. A small hollow with sizes 0.5 mm deep and 3 mm in diameter was ground out at the center of the surface of one of the detectors. The ^{125m}Te source was placed in this hollow. A sample of tellurium of high radiation purity grade was specially prepared for this experiment. A tin strip of foil with mass of 0.1g was irradiated in a reactor during one month in a flux of 10^{13} neutrons/cm^2·s. The process of production of ^{125m}Te is shown below: n+ ^{124}Sn → ^{125}Sn(β^-, $T_{1/2}$=9.7 d) → ^{125}Sb(β^-, $T_{1/2}$=2.7 y) → ^{125m}Te. After radiochemical purification a drop of sulfuric acid solution was placed in the hollow with gold coating of the HPGe detector.

After the tellurium was deposited on one of the detectors, the detector was placed on the beryllium window of a spectrometer with a Si(Li) detector. The x-ray spectrum obtained in the decay of ^{125m}Te was measured to determine the probability of L-Auger-electron emission. This value is of fundamental importance for the proposed method because it permits to distinguish between the emission of an axion from the absorption of a photon or electron in the dead layer of the detector. The probability of absorption in the detector is higher for a 27 kev X-ray (or 30 kev electron) than for a 35 keV X-ray (or 34 keV electron). At the same time, the X_L-rays accompanying such transitions are detected with nearly 100% efficiency. This gives rise to an additional intensity in the line, shifted to higher energies by 4 keV. According to the decay scheme, when an axion is emitted in the M1 transition, two peaks with energies 104.5 and 108.3 keV and the intensity ratio of 2.9 should be observed in the total spectrum. If the losses of energy are connected with absorption of particles in the dead layer of the detector, the ratio of the intensities of the indicated peaks will decrease to 2.2. This difference can be a criterion of the positive result of an observation.

After the indicated measurements were performed, the HPGe detectors were placed up against each other in a cryostat and cooled to a liquid-nitrogen temperature. The detectors had individual bias voltages of 1200 and 900 V, which were applied to the n^+ contact. The potential of their common p contact was zero. Both detectors had similar spectrometric channels: a preamplifier with resistive feedback and an uncoiled FET and an amplifier with the shaping time of 2 μs and a 4096 channel ADC. The resolution measured with respect to the 122 keV γ-line of ^{57}Co was 1.9 keV. The two channels were summed and the total signal was processed in additional ADC. The total energy spectrum from both detectors, the total spectra from each detector and four spectra corresponding to coincidences and

anticoincidences between detectors were stored in the computer memory. The two-dimensional energy spectrum was also stored in order to search for the optimal background/effect ratio.

A total of $3.5 \cdot 10^8$ decays of ^{125m}Te were detected over 150 hours of measurements. The spectrum from one detector contained 29 peaks, corresponding to different decay modes of ^{125m}Te and satellites associated with the escape of germanium X-rays from the detector. The total spectrum from the two detectors is shown in Fig.3. The background level near 104 keV was equal to $3.5 \cdot 10^5$ keV^{-1} and was determined by the tails of the electron lines associated with multiple reflections of electrons from the surface of the detectors.

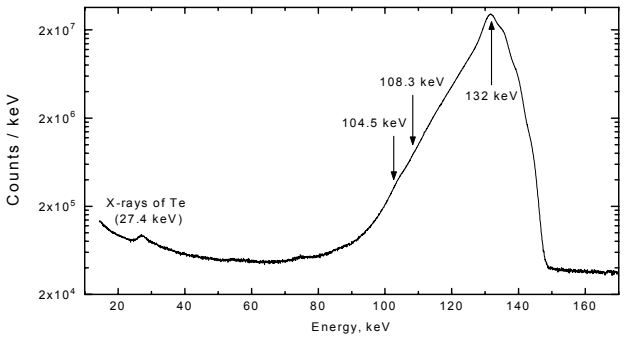

Fig.4. Spectrum of the total detected energy. The vertical lines indicate positions of the expected peaks in the case of axion emission.

The maximum likelihood method was used to find the intensities of the lines with energy 104.5-keV and 108.3-keV. The likelihood function was found from the assumption that the number of counts in each channel has a normal distribution and is a sum of an exponential function, chosen to describe the background, and the response function for the electrons, which is determined from the total spectrum

The value obtained for the ratio of the intensity of the axion radiation to the total intensity was found as $I_\alpha/I_\gamma=(4.5\pm2.5)\times10^{-6}$. It corresponds to an upper limit for probability of axion emission in M1 transition of $I_\alpha/I_\gamma(^{125m}\text{Te}) \le 0.85\times10^{-5}$ at the 90% confidence level.

We compared this result with the theoretical estimates [22]. The ratio of the probabilities ω_γ and ω_a of nuclear electromagnetic and axion transitions reaches a maximum value of 2.8×10^{-6} at m_a=22 keV. Therefore, our theoretical estimate is 3 times lower than our experimental estimate. This makes it impossible to establish a limit on the axion mass in the range (0–35) keV.

The sensitivity of our method of missing γ ray can be increased. At first the background near 104 keV must be decreased. The background level is determined mainly by the tails of the electron lines produced by backscattering of electrons from the surface of the detectors. The thickness of the dead layer of the detector and the thickness and atomic number of the conducting coating must be decreased. The contribution of the natural radioactivity to the background is almost an order of magnitude less, but using passive and active shielding can also decrease it. Increasing the measurement time and improving the resolution by using cooled FET in the preamplifiers open up additional possibilities. All these measures will make it possible to reach the sensitivity to axion mass at a level of 1 keV.

5.2 Search for the Strongly Interactive Massive Particles

The hidden masses of galaxies and galactic clusters can exist in the form of strongly interacting massive particles (SIMPs). Although those hypothetical particles have been sought both in high-altitude and in underground experiments, the masses M_H between 10^5 and 10^8 GeV and cross sections (per nucleon) between 10^{-22} and 10^{-30} cm^2 largely remain unexplored [24]). In our articles [25,26] we reported on search for SIMPs that was performed with semiconductor detectors at sea level. In this experimental environment, the background can be pushed down to a manageable level, while the energy of a SIMP is affected only by its collisions in the atmosphere. A semiconductor detector positioned on the Earth's surface executes a complex motion through a sparse cloud of SIMPs, entrained by the rotating Earth and participating in the motion about center of the Milky Way galaxy. Upon a collision of SIMPs with a nucleus in a semiconductor detector, there arises an ionization signal, which may be recorded [27,28].

Our measurements employed two semiconductor detectors based on germanium (HPGe) and silicon (Si(Li)). Thereby, we aimed at obtaining deeper insights into backgrounds and at enhancing the

sensitivity to low values of M_H. The silicon-based detector consisted of four modules that operated in the anticoincidence mode. The data-taking module had an active volume of 25 cm^3. The three additional Si(Li) modules helped suppress spurious signals due to a microphone noise. The germanium-based detector had an active volume of 115 cm^3. The detectors were placed in an evacuated cryostat surrounded by passive and active shield.

For SIMP-nucleus scattering in a semiconductor detector, the predicted form of the energy spectrum of recoil nuclei is:

$$N(E_i) = n\, T\rho/M_H \exp(-2M_t E_i R^2/3h^2) \sum (d\sigma/dE_k) f(v_k) v_k \Delta v_k \ ,$$

where n is the number of target nuclei with a mass M_A and radius R in the detector, $\rho = 0.1 - 0.7$ GeV/cm^3 is the density of SIMPs with mass M_H in the galactic halo, and T is the exposure time. The exponential factor takes into account the loss of coherence at high momentum transfers. The velocity distribution of SIMPs, $f(v)$, was assumed to have a Maxwell-Boltzmann form characterized by the root-mean-square value of v_{rms}=270 km/s and truncated at v_{esc}=600 km/s. This distribution was then rescaled to the detector rest frame at the instant of measurements. The differential cross section for SIMP - nucleus scattering, $d\sigma/dE$, was assumed to be equal to that for the scattering of a standard Dirac neutrino with a rescaled coupling constant of $G^2 = \alpha^2 G_F^2$, where G_F is the Fermi constant and α is a fitted parameter.

Through scattering in matter, a SIMP loses a part of its initial energy E_0 :

$$E = E_0 \exp(-(2/M_H) \sum_l \sigma_{Ai} d_i x_i m_{red}^2(A_i)/M_{Ai}^2).$$

Here, d_i is the density of the medium, M_{Ai} is the mass of the nucleus on which the SIMP is scattered with a cross section σ_{Ai}, x_i is the range in matter, and $m_{red}(A)$ is the reduced mass for M_{Ai} and M_H. In order that our results could be directly compared with those from the cross section, σ_A was rescaled into the cross section σ_ρ for SIMP-nucleon scattering. In Fig. 5 the closed loop *ABCDEF* in the log σ_ρ – log M_H plane bounds the region where the results of the present study rule out the existence of SIMPs (68% c.l.). Particles whose interactions with a detector material are characterized by very small cross sections, the boundary AB restricts σ_ρ to be less than 10^{-39}– $10^{-31}$$cm^2$. Relatively small values of M_H are restricted from above by the boundary *AF*: a SIMP with $M_H \leq 30$ GeV would deposit less than energy threshold

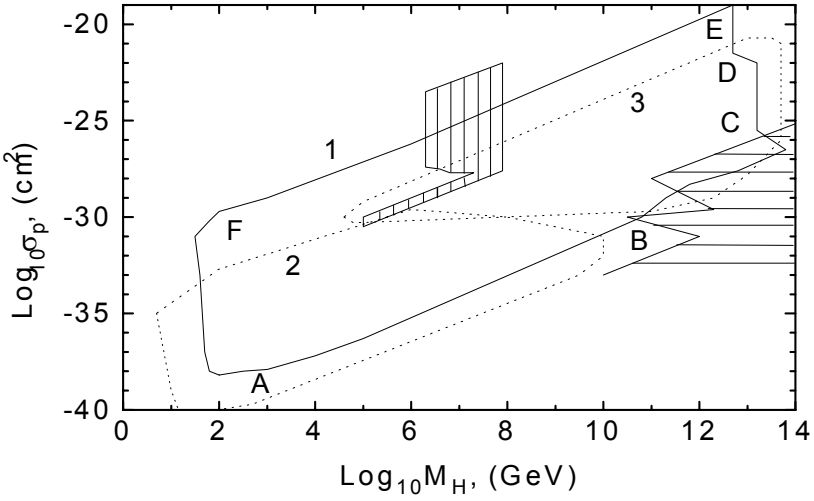

Fig. 5. Region ABCDE where the existence of SIMPs is ruled out

of the detectors. In the allowed region above the boundary *EF*, SIMPs have lost too much energy in the atmosphere to be detectable under our experimental conditions. The broken line *BCDE* represents a lower limit on M_H for superheavy SIMPs.

References

1. M.B.Voloshin, M.I.Vysotsky, L.B.Okun, Zh.Eksp.Teor.Fiz., **91**, 754 (1986).
2. A.V.Kyuldiev, Nucl.Phys., **B234**, 384 (1984).
3. P.Vogel, J.Engel, Phys.Rev., **D39**, 3378, (1989).
4. A.V.Derbin, preprint PNPI, **N1765**, (1992).
5. A.V.Derbin, Physics of Atomic Nuclei, 57, 222 (1994) (Yadernaya Fizika, 57, 236 (1994).
6. A.V.Derbin, Proceedings of XXXII Winter School of PNPI, **1**, 97 (1998).
7. A.V.Derbin, Elementary Particles and Atomic Nuclei (EChAYa), **32**, N3, (2001).
8. V.I.Kopeikin, L.A.Mikaelayn, V.V.Sinev, Yad. Fiz., 60, 230, (1997).
9. J.J.Simpson, Phys.Rev.Lett. **54**, 1891 (1985).
10. A.V.Derbin, A.I.Egorov, V.N.Muratova et al., JETP Lett., **58**, 1 (1993).
11. A.V.Derbin, A.I.Egorov, S.V.Bakhlanov and V.N.Muratova, JETP Lett., **66**, 88 (1997).
12. O.I.Sumbaev, Sov.Phys.Dokl. **36**, 165 (1991) and priv. comm.
13. V.M.Lobashev, V.N.Aseev, A.I.Belesev et al., Nucl.Phys. B (Proc.Suppl.), **77**, 327 (1999)ю
14. A.M.Apalikov, S.D.Boris, A.I.Golutvin et al., JETP Lett., **42**, 289 (1985).
15. J.Markey, F.Boehm, Phys.Rev., **32**, 2215 (1985).
16. K.Schreckenbach, G.Golvin, F. von Feilitzsch, Phys.Lett. **B129**, 265 (1983).
17. A.S.Barabash, F.T.Avignone, J.I.Collar et al., Phys.Lett., **B345**, 408 (1995).
18. A.V.Derbin, A.I.Egorov, V.N.Muratova, S.V.Bakhlanov, Physics of Atomic Nuclei, **59**, 2037 (1996).
19. A.R.Zhitniskii, Yad.Fys., **31**, 497 (1980).
20. M.A.Shifman, A.I.Vainstein, V.I.Zakharov, Nucl.Phys., **B166**, 493 (1980).
21. M.Minowa, Y.Inoue, T.Asanuma, M.Imamura, Phys.Rev.Lett., **71**, 4120 (1993).
22. A.V.Derbin, A.I.Egorov, I.A.Mitropol'skii, V.N.Muratova et al., JETP Lett., **65**, 605 (1997).
23. A.V.Derbin, A.I.Egorov, I.A.Mitropol'skii, V.N.Muratova et al., Preprint PNPI **N2397** (2000).
24. G.D.Starkman, A.Gould, R.Esmailzadeh et al., Phys.Rev., **D41**, 3594 (1990).
25. A.V.Derbin, A.I.Egorov, S.V.Bakhlanov, V.N.Muratova, Physics of Atomic Nuclei, **62**, 1886 (1999).
26. A.V.Derbin, A.I.Egorov, S.V.Bakhlanov, V.N.Muratova, preprnt PNPI, N **2254** (1998).
27. A.K.Drukier, L.Stodolsky, Phys.Rev., **D30**, 2295 (1984).
28. M.W.Goodman, E.Witten, Phys.Rev.., **D31**, 2059 (1985).